THERMONEUTRAL HOUSING DID NOT IMPACT THE COMBINED EFFECTS OF EXTERNAL LOADING AND RALOXIFENE ON BONE MORPHOLOGY AND MECHANICAL PROPERTIES IN GROWING FEMALE MICE

by

Carli A. Tastad

A Thesis

Submitted to the Faculty of Purdue University

In Partial Fulfillment of the Requirements for the degree of

Master of Science in Biomedical Engineering

Department of Biomedical Engineering

Indianapolis, Indiana

December 2020

THE PURDUE UNIVERSITY GRADUATE SCHOOL
STATEMENT OF COMMITTEE APPROVAL

Dr. Joseph M. Wallace, Chair

Department of Biomedical Engineering

Dr. Matthew R. Allen

Department of Anatomy, Cell Biology, and Physiology

Dr. Jiliang Li

Department of Biology

Approved by:

Dr. Joseph M. Wallace

TABLE OF CONTENTS

LIST OF TABLES

LIST OF FIGURES

LIST OF ABBREVIATIONS

BMD	Bone Mineral Density
RAL	Raloxifene
SERM	Selective Estrogen Receptor Modulator
DXA	Duel-Energy X-Ray Absorptiometry
TNZ	Thermoneutral Zone
CON	Control
µCT	Microcomputed Tomography
ROI	Region of Interest
BV/TV	Bone Volume Fraction
TMD	Tissue Mineral Density
I_{max}	Maximum Moment of Inertia
I_{min}	Minimum Moment of Inertia
Disp.	Displacement

ABSTRACT

Raloxifene is an FDA-approved selective estrogen receptor modulator (SERM) that improves tissue quality by binding to collagen and increasing the bound water content in the bone matrix in a cell-independent manner. In this thesis, active tissue formation was induced by non-invasive external tibial loading in female mice and combined with raloxifene treatment to assess their combined effect on bone morphology and mechanical properties. Thermoregulation is an important factor that could have physiological consequences on research outcomes, and was introduced as an additional experimental factor in this study. We hypothesized that by removing the mild cold stress under which normal lab animals are housed, a metabolic boost would allow for further architectural and mechanical improvements as a result of the combination of tibial loading and raloxifene treatment. Ten week old female C57BL/6J mice were treated with raloxifene, underwent tibial loading to a strain level of 2050με and were housed in thermoneutral conditions (32°C) for 6 weeks. We investigated bone morphology through microcomputed tomography (μCT) and mechanical properties via four-point bending and fracture toughness testing. Results indicated a combined improvement by external loading and raloxifene on geometry, particularly in the cancellous region of the bone, and also in bone mechanics leading to greater improvements than either treatment individually. Temperature did not have a robust impact on either bone architecture or mechanical integrity.

1. INTRODUCTION

1.1 Bone Overview

Bone is a dynamic living structure that serves many functions in the body. Bone has a complex, hierarchal organization with each multiscale level contributing to its overall mechanical integrity. The fractal-like organization begins with a composite matrix at the nanoscale level comprised of carbonated apatite mineral, type I collagen, and non-collagenous proteins. By weight, bone is composed of approximately 65% mineral, 25% organic (primarily type I collagen), and 10% water. Mineral provides bone with its stiffness and collagen provides its resilience and ductility. Collagen has a trimeric helical structure consisting of two α1 chains and a single α2 chain. Each chain comprises repeating units of Glycine-X-Y where X and Y are often occupied by proline and hydroxyproline. Hydroxyproline is important for collagen because its hydroxyl group is essential for hydrogen bonding with water molecules. Water in bone is either bound to the composite matrix or free to flow through vascular channels. As mineral content increases, water content typically decreases proportionally. This is important for mechanical behavior because a highly mineralized bone is stiffer due to its mineral content, but also because it has less water. Despite increased stiffness and strength, this bone also tends to be more brittle, lacking tissue toughness, and can break easier due to an inability to tolerate the development of energy-dissipating damage. [1]

The microscopic organization of bone supports the cells that are essential to producing and maintaining its structure. Osteoblasts, osteoclasts, and osteocytes each play an integral role in bone remodeling and modelling. Osteoclasts are responsible for bone resorption and osteoblasts are the cells that form new bone. Osteoblasts that become trapped in the matrix during bone formation differentiate into and interconnected network of osteocytes. Collagen forms the template for mineral which exists within and between collagen fibrils. Layers of this mineralized construct form discreet sheets called lamellae. Lamellae layer upon each other to create the macroscopic organization of bone which can be divided into dense cortical bone and more porous cancellous bone made of trabecular struts. [1]

Bone mass and size are obvious and well-known contributors to the mechanical behavior of bone, but work in combination with the intrinsic quality of bone tissue to influence bone's overall

mechanical integrity. Tissue quality refers to anything contributing to the inherent chemical or physical properties of bone notwithstanding bone mass or macroscopic structure. [2]

1.2 Raloxifene

Skeletal fragility and increased fracture are the result of several bone diseases and disorders. Current diagnostic tools and treatment options for skeletal fragility focus primarily on bone mass and bone mineral density (BMD), with little regard given to bone tissue quality. Raloxifene (RAL) is an FDA-approved selective estrogen receptor modulator (SERM) used to treat osteoporosis in post-menopausal women. [3] Raloxifene is a non-steroidal benzothiophene derivative that inhibits bone resorption by reducing osteoclast activity and reduces the rate of bone loss by binding and signaling through estrogen receptors on osteoblasts. [4] The efficacy of RAL is well demonstrated, with a clinical reduction in fracture risk by 50% with only modest changes in remodeling and BMD. [5,6] The lack of robust mass-based improvements suggests that changes in mechanical integrity are potentially driven by changes in tissue quality.

Although the exact mechanism by which RAL reduces fracture risk is unknown, several pre-clinical studies have demonstrated the ability of RAL to improve material-level properties in bone independent of BMD. These improvements may not be detectable clinically by dual-energy x-ray absorptiometry (DXA), which measures bone mineral content and mass. [7,8,9] Further work has shown that RAL binds to collagen through its hydroxyl groups and increases bone tissue hydration by increasing the bound water content at the collagen-mineral interface. The increased water content at the matrix interface alters the transfer of load between the collagen and hydroxyapatite mineral, leading to reduced strains in the mineral and increased whole-bone toughness and fatigue life. [10,11,12] These data would suggest that RAL modifies the bone matrix independent of BMD, thus improving material-level properties of the bone and offering a unique opportunity to enhance bone mechanical properties in a cell-independent manner.

1.3 Mechanical Loading

Osteocytes are mechanosensory cells that are able to detect changes in the bone mechanical environment and direct osteoclast and osteoblast cell activity. The Mechanostat explains that an anabolic response to loading in bone is threshold driven. When a load is applied, the osteocytes

direct osteoblasts to form new bone. Intrinsic loading (forces are imposed by the animals own activities, e.g. exercise) and extrinsic loading are different models to apply a load to the bone, resulting in increased bone mass. [13,14,15,16] Extrinsic loading allows for control over loading parameters to focus on the mechanisms underlying a response to mechanical stimulation. Forces are imposed on the skeletal element in extrinsic loading models and can be either invasive or non-invasive. Non-invasive loading models are appealing because they are technically simpler, cheaper, and are not influenced by the healing process. One of the first such models used was a bending model which subjects the tibia to four-point bending. This method is useful for studying endocortical adaptation, but is not ideal for periosteal bone formation since a woven bone response is typically elicited by the loading points being in contact with the bone's surface. Cantilever bending is another loading model in which the proximal tibia is fixed and an actuator pushes the distal end of the tibia medially resulting in mediolateral bending. Cantilever bending can be useful for both endocortical and periosteal adaptation investigations. Ulnar axial loading is the most widely used in vivo loading model in rodents in which the forearm is secured vertically with the elbow and flexed wrist within two cup fixtures that are mounted to platens of a material testing machine. Compressive forces are applied and transmitted to the ulnar diaphysis through the skin, fascia, and articular cartilage, and ulnar metaphyseal bone. The natural curvature of the bone results in a mediolateral bending moment. Animals are allowed normal activity between loading bouts. The ulnar model has been adapted for the tibia in compressive tibial loading. Advantages tibial loading has over ulnar loading are that force is never directly applied to the bone under study and trabecular bone adaptation in the proximal tibia can be studied. Tibial loading is utilized in the current study to investigate bone adaptation in both cancellous and cortical regions. [17]

1.4 Thermoregulation

Mice are the most commonly utilized animal model for pre-clinical biomedical research. One factor that is not often considered, but is becoming better appreciated, is that the thermal physiological characteristics of mice may impact seemingly unrelated characteristics or endpoints in these models. The thermoneutral zone (TNZ) is the range of temperatures across which resting metabolic rate of heat production is at equilibrium with the animal's evaporative heat loss to the surrounding environment. TNZ is determined by body size and weight, morphology, condition, and resting metabolic rate, and therefore, spans only 1-3 °C in mice due to the large surface-to-

volume ratio and meager body insulation. The lower and upper critical temperatures for a laboratory mouse is 30 and 32 °C, respectively, outside of which the mouse must engage in heating or cooling adjustments that can be behavioral and/or physiological (thermogenesis – shivering/non-shivering). [18,19] Therefore, laboratory mice housed under standard temperatures are subject to mild cold stress which has been attributed to physiologic changes. Since metabolism in these mice is altered to compensate, it is possible that the response of mice to stimuli which requires further metabolic changes could be blunted.

While mice are often used in bone disease research, the temporal pattern of bone loss in long bones is different between mice and humans. In mice, cancellous bone loss occurs prior to skeletal maturity and concurrently with bone elongation [20]. This bone loss during growth does not occur in humans. Bone loss occurs after skeletal maturity in humans driven by a remodeling imbalance. The mechanisms mediating premature bone loss are not well established, however, C57BL/6J mice housed at thermoneutral temperature did not exhibit the cancellous bone loss in distal femur that is typically noted in standard temperature-housed mice, suggesting housing temperature is a critical factor. [21,22]

1.5 Gap and Plan of Attack

Current standards for care of lab mice typically house those mice at room temperature (22 °C), below metabolic TNZ and affecting the physiological properties being studied. This study is expanding on a previous study performed in the lab [23] in which RAL was administered during a period of active tissue formation (tibial loading) to evaluate mechanical changes. Treatment with RAL during a period of active tissue formation may allow for additional mechanical enhancements by increasing hydration in this newly forming tissue prior to mineralization. Active tissue formation can be induced by mechanically stimulating a bone or bones, with targeted loading of limbs being one way to accomplish this. [24,25,26] Given the modest impacts of RAL in combination with tibial loading that were observed, the addition of thermoneutral housing at 32°C is being considered here.

By removing the mild cold stress placed on the animals, it was hypothesized that housing mice in a thermoneutral condition would facilitate an additive effect on bone mechanics in mice undergoing tibial loading and RAL treatment. Female mice were chosen based on the clinical use of raloxifene in humans, and also because the mechanical impacts were less pronounced in females

in the previous study. By housing mice within their TNZ, it is expected that there will be a metabolic boost allowing loading and RAL to further enhance the mechanical properties in bone.

2. MATERIALS AND METHODS

2.1 Animals and Treatment

All protocols and procedures were performed with prior approval from the Indiana University – Purdue University Indianapolis School of Science Institutional Animal Care and Use Committee (Protocol SC296R). Female C57BL/6J mice were purchased from Jackson Laboratory (Bar Harbor, ME) at 9 weeks of age and allowed one week to acclimate to the animal housing facility. Mice were randomly assigned into four weight-matched groups (n = 20 per group): Standard-Control (Standard-CON), Standard-RAL, Thermoneutral-CON, and Thermoneutral-RAL. Two groups of mice were housed in either standard room temperature (22°C) or thermoneutral temperature (32°C) conditions, starting at 10 weeks of age and continuing for 6 weeks. One group in each housing condition was injected subcutaneously with RAL (0.5 mg/kg; 5x/week) in a 10% hydroxyl-β-cyclodextrin solution. This dosage was chosen based on previous research showing efficacy *in vivo*. [27,28,29] Mice were weighed weekly. Untreated controls were also included in each housing condition. At 16 weeks of age, the mice were euthanized by CO_2 inhalation followed by cervical dislocation. Tibiae were harvested, stripped of soft tissue, length was measured with calipers, and then they were wrapped in saline-soaked gauze and stored at -20°C until needed.

2.2 In vivo Tibial Loading

Starting at 10 weeks of age, each mouse underwent compressive tibial loading 3x/week for 6 weeks. Prior to the start of loading, a strain calibration study was performed on five mice to determine the average force necessary to induce a tensile strain of 2050 με on the anteromedial surface, a level shown to be osteogenic in mice of this age and sex. [30] Mice were anesthetized (2% Isoflurane) and their left limb cyclically loaded in compression, leaving the contralateral limb as an internal control. Each loading profile consisted of 2 cycles at 4 Hz to a maximum load of 11.2 N, followed by a 1-second rest at 2 N, repeated 110 times for a total of 220 compressive cycles per day.

2.3 Microcomputed Tomography (μCT) and Architectural Analysis

To determine the effects of housing, loading, and treatment on bone architecture, both tibiae from each mouse were scanned *ex vivo* (three bones at a time) using an isotropic voxel size of 10 μm (Skyscan 1172, Bruker). Bones were scanned through a 0.5 mm Al filter (V = 60kV, I = 167μA) with a 0.7-degree angle increment and two frames averaged. Images were reconstructed (nRecon) and rotated (Data Viewer) before calibrating to hydroxyapatite-mimicking phantoms. (0.25 and 0.75 g/cm^3 Ca-HA). A 1 mm trabecular region of interest (ROI) was selected at the proximal metaphysis (extending distally from the most distal portion of the growth plate), and then quantified using CT Analyzer (CTAn). A 0.1 mm ROI was selected at approximately 37.5% length of the tibia, then analyzed with a custom MATLAB script. [30]

2.4 Four-Point Bending Mechanical Testing to Failure

Tibiae from twelve mice per group were randomly selected for four-point bend tests to failure (lower support span at 9 mm, upper loading span at 3 mm), with the medial surface in tension. The bones were loaded at a displacement control rate of 0.025 mm/s while the sample remained hydrated with phosphate buffered saline (PBS). Cross-sectional cortical properties at the center of the load span were obtained from μCT images as described above. These properties were used to map load-displacement data into stress-strain data using standard engineering equations as previously reported to estimate tissue level properties. [31] Two bones in the standard control group and one bone from the thermoneutral control group were removed from analysis due to abnormal mechanical curves caused by rotation during testing. Contralateral limbs were also removed from the analysis.

2.5 Fracture Toughness Testing

Tibiae from the remaining eight mice from each group were used for fracture toughness testing using a linear elastic fracture mechanics approach. [32,33] A notch was made through the anteromedial surface of the tibia, at approximately 50% of the bone length, using a straight razor blade lubricated with a 1 μm diamond suspension. The tibiae were notched into the medullary cavity, not exceeding the bone's midpoint. One bone each from the standard and thermoneutral control groups was broken during notching and thus removed from analysis. Additionally, the

contralateral limbs were not considered for analysis. The bones were then tested to failure in three-point bending at a displacement rate of 0.001 mm/s with the notched surface in tension and the notched site directly below the load point.

After mechanical testing, the bones were cleansed of marrow and dehydrated in an ethanol gradient (70-100%) and then dried overnight in a vacuum desiccator. The proximal cross-sectional fracture surface of the dehydrated bones was sputter-coated with gold and then imaged with scanning electron microscopy (SEM, JEOL7800f). The SEM images revealed the angles of stable and unstable crack growth, which were used in conjunction with geometric properties from μCT data at the notch site to calculate the stress intensity factors for crack initiation, maximum load, and fracture instability, using a custom MATLAB script.

2.6 Statistical Analysis

Repeated measures (RM) three-way ANOVA tests were used to statistically analyze main effects of housing temperature, treatment, and loading. A two-way ANOVA test was used to statistically analyze main effects of housing and treatment for body weights. If a significant interaction occurred, the ANOVA was followed by a Tukey post-hoc test. Analysis was performed using GraphPad Prism (v.8) with a significance level at $\alpha = 0.05$. Effect size was calculated by dividing two population mean differences by their pooled standard deviation in order to quantify the strength of the differences between two groups. Effects sizes were calculated between CON and RAL in non-loaded animals to determine the effect size for RAL, between non-loaded and loaded in CON animals to determine the effect size for loading, and between non-loaded, CON and loaded, RAL to determine the combined effect size.

3. RESULTS

3.1 Body Weight and Tibial Length

At the beginning of the study, mice were placed in weight-matched groups (19.4 ± 0.97 g). Each group increased weight throughout the duration of the study: standard-CON (+7.3%), standard-RAL (+3.2%), thermoneutral-CON (+3.9%), thermoneutral-RAL (+1.5%). There was a significant decrease in weight due to thermoneutral housing temperature (p=0.0196) and RAL treatment (p=0.004), but these differences were modest and significance was likely driven by the large sample sizes rather than a biologically relevant difference **(Fig-1A)**. Tibial length was also significantly decreased due to RAL (p=0.0306), but increased due to loading (p=0.0022) **(Fig-1B)**. These changes were also modest.

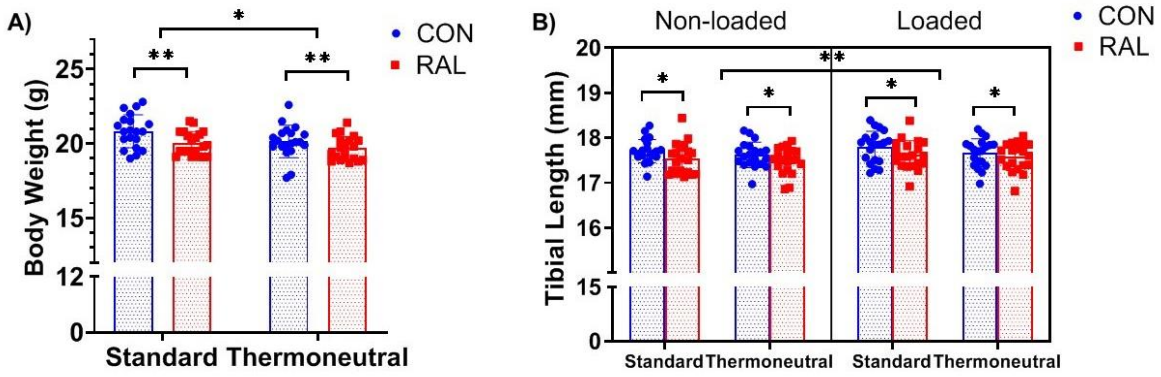

Figure 1. Final body weight (g) and final tibial length (mm) (n=20 per group). **A)** Final body weights decreased with temperature and RAL treatment. 2-way ANOVA performed with main effects of treatment and temperature: ** p=0.004, * p=0.0196. **B)** Left tibiae (loaded) were longer than right tibiae (non-loaded). 3-way ANOVA performed with main effects of temperature, loading, and treatment: ** p=0.0022, * p=0.0306.

3.2 Cancellous Architecture Improves Due to Loading and RAL Treatment

Both loading and RAL improved trabecular architecture and mineralization in all properties investigated. Raloxifene significantly increased bone volume fraction (BV/TV, p<0.0001) **(Fig-2A)**. An interaction effect from loading x temperature was present in BV/TV (p=0.0074). The increased effect due to loading is clear in all post-hoc analyses, with temperature contributing modestly to any effect. The effect due to RAL (effect size=1.837) was similar to that of loading

(effect size=1.523), at standard temperature, but the improvements were additive in nature (combined effect size=3.032). At thermonetural temperature, the effect sizes of RAL, loading, and combined were 1.583, 2.813, and 3.655, respectively. The effect size of RAL, loading, and temperature combined was 3.635, which did not increase from the combined RAL and loading alone effect sizes, helping to emphasize the lack of a temperature effect. The increase in BV/TV was driven by an increase in trabecular thickness (Tb.Th) and trabecular number (Tb.N) and a decrease in trabecular spacing (Tb.Sp) due to both loading and RAL **(Table 1)**. Thermoneutral temperature decreased trabecular thickness (p=0.0297). A 3-way interaction between temperature, loading, and treatment occurred for tissue mineral density (tTMD, p=0.0083) **(Fig-2B)**. The statistical effect size reinforced the similar contribution of RAL (1.551, 0.517) and loading (1.939, 0.772) at standard and thermoneutral temperatures, respectively. The effects were also greater combined in tTMD, as shown by the increased effect sizes of RAL+loading (standard-2.623, thermoneutral-1.849). Bone mineral density (tBMD) was also significantly increased by loading ($p<0.0001$) and RAL ($p<0.0001$), but temperature had no effect (p=0.5026)

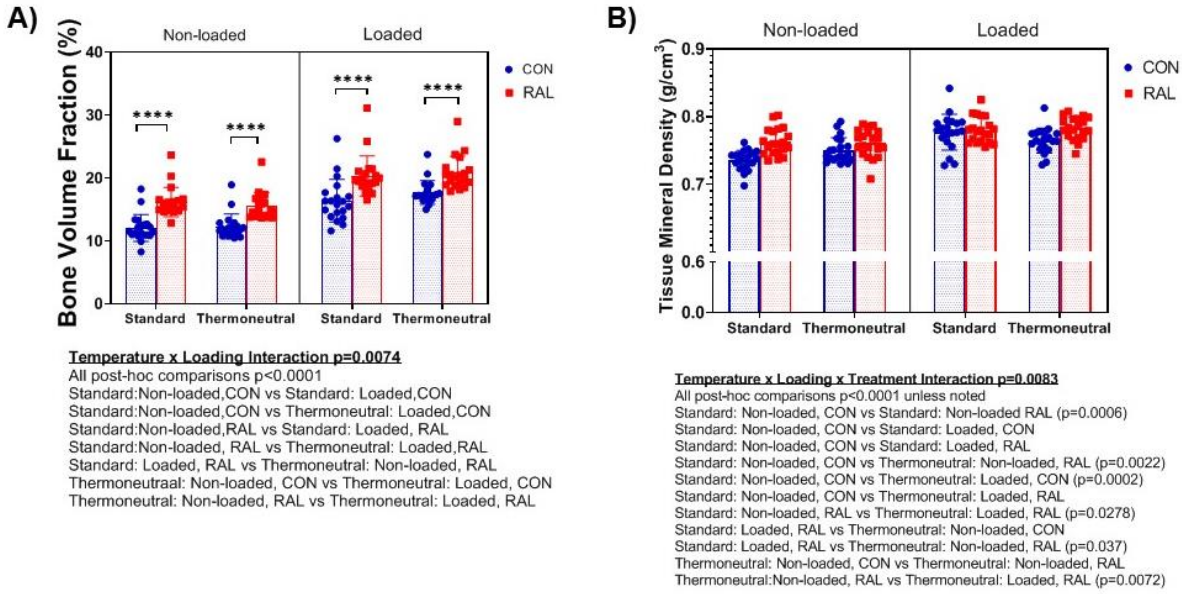

Figure 2. Trabecular geometry of right (non-loaded) and left (loaded) tibiae (n=20 per group). **A)** Bone volume fraction increased significantly due to RAL treatment. **B)** A three way interaction effect occurred for tissue mineral density. **** $p<0.0001$.

Table 1. Trabecular properties of right (non-loaded) and left (loaded) tibiae (n=20 per group). RM 3-way ANOVA test with temperature (temp), loading (load), and treatment (treat) main effects.

Trabecular Property	Standard				Thermoneutral				P-value						
	Non-loaded		Loaded		Non-loaded		Loaded		Temp	Load	Treat	Temp x Load	Temp x Treat	Load x Treat	Temp x Load x Treat
	CON	RAL	CON	RAL	CON	RAL	CON	RAL							
Tb.Th (µm)	6.14 ± 0.21	6.73 ± 0.26	7.68 ± 0.71	7.91 ± 0.42	6.14 ± 0.19	6.61 ± 0.20	7.39 ± 0.31	7.82 ± 0.30	**0.0297**	**<0.0001**	**<0.0001**	0.2884	0.7485	0.0937	0.1595
Tb.Sp (µm)	23.66 ± 1.98	22.68 ± 1.51	23.1 ± 2.85	21.55 ± 1.65	23.58 ± 1.67	22.23 ± 1.68	21.52 ± 1.7	21.27 ± 1.93	0.1352	**<0.0001**	**0.0107**	**0.0465**	0.5541	0.4041	**0.0129**
Tb.N (1/µm)	0.02 ± 0	0.02 ± 0	0.02 ± 0	0.03 ± 0	0.02 ± 0	0.02 ± 0	0.02 ± 0	0.03 ± 0	0.2550	**<0.0001**	**<0.0001**	**0.0003**	0.4093	0.3230	0.3968
BMD (g/cm^3 HA)	0.15 ± 0.02	0.20 ± 0.002	0.19 ± 0.03	0.23 ± 0.03	0.16 ± 0.02	0.19 ± 0.002	0.20 ± 0.02	0.24 ± 0.03	0.6016	**<0.0001**	**<0.0001**	0.1000	0.4876	0.7306	0.3543

Significant Post-hoc Tukey Comparisons

Tb.Sp	**p-value**
Standard: Non-loaded, CON vs Standard: Loaded, RAL	0.0139
Standard: Non-loaded, CON vs Thermoneutral: Loaded, CON	0.0117
Standard: Non-loaded, CON vs Thermoneutral: Loaded, RAL	0.0029
Standard: Non-loaded, RAL vs Standard: Loaded, RAL	0.0201
Standard: Loaded, RAL vs Thermoneutral: Non-loaded, CON	0.0214
Thermoneutral: Non-loaded, CON vs Thermoneutal: Loaded, CON	<0.0001
Thermoneutral: Non-loaded, CON vs Thermoneutral: Loaded, RAL	0.0047
Tb.N	**p-value**
Standard: Non-loaded, CON vs Standard: Loaded, CON	0.0125
Standard: Non-loaded, CON vs Thermoneutral: Loaded, CON	0.0032
Standard: Non-loaded, RAL vs Standard: Loaded, RAL	0.0191
Thermoneutral: Non-loaded, CON vs Thermoneutral: Loaded, CON	<0.0001
Thermoneutral: Non-loaded, RAL vs Thermoneutral: Loaded RAL	<0.0001

3.3 Cortical Geometry at the Tibial Proximal-Mid Diaphysis is Improved by Loading and RAL Treatment

Cortical bone mass showed effects of loading in all properties investigated. Similar to the trabecular region, there were combined effects of loading and RAL, evident by significant loading x treatment interaction effects, in total area ($p<0.0001$), marrow area ($p=0.0127$), bone area (0.0057), I_{max} ($p=0.0001$), and I_{min} ($p=0.0355$). Loading and RAL both increased each property **(Table 3)**. By assessing the statistical effect sizes, the main contributor to the improvement of the geometric properties was loading since the effect sizes are much greater, regardless of the housing temperature. The combined effect sizes are still greater in most properties, indicating the combination is greater than either single effect **(Table 2)**. Loading and RAL both significantly increased cortical thickness ($p<0.0001$ for both) **(Fig-3A)**. Loading also significantly decreased tissue mineral density (TMD, $p<0.0001$) **(Fig-3B)**. Bone area density was significantly increased by loading ($p<0.0001$) and RAL ($p=0.0021$) and decreased by temperature ($p=0.0022$). Temperature significantly decreased bone area ($p=0.0254$), cortical thickness ($p=0.005$), and I_{max} ($p=0.0034$), and increased TMD ($p=0.0035$) **(Fig-3B)**. These impacts were modest compared to the robust loading and treatment responses.

Table 2. Cortical property effect sizes increase when loading and RAL are combined indicating the combination has a greater effect than either single effect.

Geometric Property	Standard Temperature			Thermoneutral Temperature		
	RAL	Loading	Combined	RAL	Loading	Combined
Total Area	0.601	2.577	2.783	1.360	3.005	3.777
Marrow Area	0.090	0.817	0.451	0.394	0.715	0.647
Bone Area	0.721	2.994	3.297	1.701	3.671	4.618
Bone Area Density	0.523	1.155	1.998	0.579	1.671	2.339
Cortical Thickness	0.656	2.200	2.738	1.271	2.759	3.537
I_{max}	0.480	2.404	2.632	1.225	3.489	3.311
I_{min}	0.535	2.448	2.536	1.247	2.511	3.739
TMD	0.115	-0.543	-0.937	-0.198	-1.209	-0.744

Table 3. Cortical properties of right (non-loaded) and left (loaded) tibiae (n=20 per group). RM 3-way ANOVA test with temperature (temp), loading (load), and treatment (treat) main effects.

Cortical Property	Standard				Thermoneutral				p-value						
	Non-loaded		Loaded		Non-loaded		Loaded		Temp	Load	Treat	Temp x Load	Temp x Treat	Load x Treat	Temp x Load x Treat
	CON	RAL	CON	RAL	CON	RAL	CON	RAL							
Total area (mm^2)	1.26 ± 0.07	1.30 ± 0.07	1.43 ± 0.06	1.43 ± 0.05	1.24 ± 0.06	1.32 ± 0.05	1.41 ± 0.05	1.43 ± 0.04	0.6868	**<0.0001**	**0.0043**	0.4527	0.2365	**<0.0001**	0.5296
Marrow Area (mm^2)	0.49 ± 0.03	0.49 ± 0.03	0.52 ± 0.05	0.50 ± 0.03	0.50 ± 0.03	0.51 ± 0.04	0.52 ± 0.04	0.52 ± 0.03	0.0780	**<0.0001**	0.8589	0.3645	0.3602	**0.0127**	0.9386
Bone Area (mm^2)	0.77 ± 0.06	0.81 ± 0.05	0.91 ± 0.03	0.93 ± 0.04	0.75 ± 0.04	0.81 ± 0.03	0.89 ± 0.04	0.91 ± 0.03	**0.0254**	**<0.0001**	**<0.0001**	0.9864	0.3358	**0.0057**	0.4614
Bone Area Density (%)	61.36 ± 1.87	62.37 ± 1.97	63.69 ± 2.15	64.94 ± 1.7	60.02 ± 1.70	61.18 ± 2.25	63.02 ± 1.88	63.89 ± 1.61	**0.0022**	**<0.0001**	**0.0021**	0.4424	0.8679	0.9651	0.6203
I_{max} (mm^4)	0.20 ± 0.03	0.22 ± 0.03	0.27 ± 0.03	0.27 ± 0.02	0.18 ± 0.02	0.21 ± 0.01	0.26 ± 0.02	0.26 ± 0.02	**0.0034**	**<0.0001**	0.0585	0.7573	0.6017	**0.0001**	0.3859
I_{min} (mm^4)	0.07 ± 0.01	0.08 ± 0.01	0.10 ± 0.01	0.10 ± 0.01	0.07 ± 0.01	0.08 ± 0.01	0.09 ± 0.01	0.10 ± 0.01	0.5483	**<0.0001**	**0.0007**	0.3130	0.1056	**0.0355**	0.9326

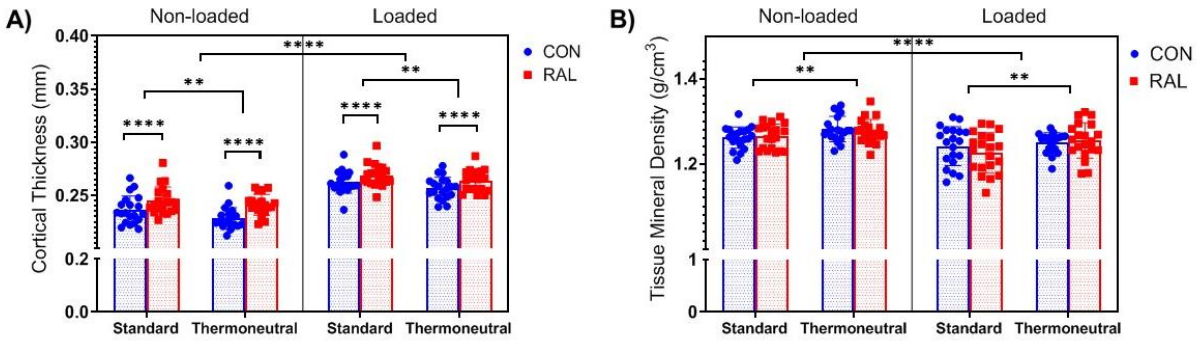

Figure 3. Cortical properties of right (non-loaded) and left (loaded) tibiae (n=20 per group). **A)** Cortical thickness was increased due to loading and RAL and decreased due to temperature. **** p<0.0001, ** p=0.005. **B)** Tissue mineral density was decreased due to loading and increased due to temperature. **** p<0.0001, ** p=0.0035.

3.4 Mechanical Properties and Fracture Toughness are Primarily Impacted by Loading

Four-point bending to failure showed an effect of loading on both whole bone (ultimate force, failure force, ultimate displacement: all p<0.0001, postyield work: p=0.0241, and total work: p=0.0186) and tissue level (toughness: p=0.0426, ultimate stress: p=0.004, failure stress: p=0.0016, ultimate strain: p<0.0001) mechanical properties. Each mechanical property was increased by loading. Treatment impacted fewer mechanical properties. RAL increased ultimate force (p=0.0092), stiffness (p=0.0054), postyield work (p=0.0131), total work (p=0.0068), and toughness (p=0.0393) and decreased ultimate stress (0.0420). The statistical effect sizes indicate a greater combination effect between loading and RAL for properties that were increased with RAL treatment. Temperature had no significant effect on mechanical properties.

Loading significantly increased the stress intensity factor for crack initiation (p=0.0012). There was an interaction effect due to loading x treatment for the stress intensity factor for the maximum load. Post-hoc analysis indicated there was only a significant effect between standard: non-loaded, CON vs thermoneutral: loaded, RAL (p=0.0069). A loading x treatment interaction effect was present in the stress intensity factor for fracture instability (p=0.0344), but there were no significant post-hoc effects. Neither RAL nor temperature had any significant effects on fracture toughness on their own.

Table 4. Structural mechanical properties from 4-point bending of right (non-loaded) and left (loaded) tibiae.

Property	Standard				Thermoneutral				p-value						
	Non-loaded		Loaded		Non-loaded		Loaded								
	CON	RAL	CON	RAL	CON	RAL	CON	RAL	Temp	Load	Treat	Temp x Load	Temp x Treat	Load x Treat	Temp x Load x Treat
Yield Force (N)	15.5 ± 2.6	15.2 ± 1.1	15.3 ± 3.5	16.1 ± 3.8	14.3 ± 2.1	14.3 ± 2.1	14.3 ± 4.7	17.5 ± 5.0	0.8146	0.2374	0.1086	0.7089	0.1391	0.3136	0.2580
Failure Force (N)	9.6 ± 4.3	11.0 ± 3.8	14.3 ± 3.5	12.5 ± 3.2	8.9 ± 3.6	10.5 ± 3.2	13.5 ± 4.7	16.8 ± 6.4	0.6454	**<0.0001**	0.2081	0.2637	0.1076	0.9538	0.1134
Ultimate Disp. (µm)	310.5 ± 53.3	309.5 ± 24.9	386.0 ± 64.4	350.7 ± 59.3	315.7 ± 22.1	326.8 ± 30.2	382.3 ± 62.6	376.0 ± 130.4	0.2352	**<0.0001**	0.7738	0.8310	0.7527	0.2484	0.6022
Disp. to Yield (µm)	261.4 ± 71.5	241.7 ± 27.7	242.2 ± 47.4	237.4 ± 49.8	246.4 ± 33.0	239.1 ± 20.1	224.2 ± 71.9	217.8 ± 25.6	0.2256	0.4245	0.3548	0.1786	0.9043	0.5484	0.6713
Postyield Disp. (µm)	490.8 ± 250.9	515.0 ± 205.9	506.8 ± 286.6	509.7 ± 100.3	574.8 ± 297.9	497.5 ± 170.0	513.4 ± 120.4	498.7 ± 108.4	0.3671	0.3789	0.7537	0.9567	0.2131	0.4065	0.9806
Total Disp. (µm)	752.2 ± 242.4	756.7 ± 211.5	749.0 ± 267.5	747.1 ± 91.3	821.2 ± 304.3	736.6 ± 163.0	737.6 ± 127.8	716.5 ± 106.2	0.4975	0.3098	0.8971	0.8134	0.1900	0.5002	0.9096
Stiffness (n/mm)	67.5 ± 10.8	71.4 ± 12.3	70.2 ± 9.9	75.7 ± 10.7	65.6 ± 10.9	73.1 ± 7.3	73.0 ± 17.9	91.7 ± 29.3	0.2950	**0.0476**	**0.0054**	0.1711	0.0734	0.0631	0.2978
Work to Yield (mJ)	2.2 ± 1.0	1.9 ± 0.3	2.0 ± 0.8	2.1 ± 0.9	1.9 ± 0.5	2.0 ± 0.4	1.8 ± 0.9	2.0 ± 0.6	0.5247	0.4947	0.7883	0.3055	0.5615	0.9155	0.6343
Postyield Work (mJ)	5.4 ± 2.3	6.7 ± 2.9	7.9 ± 4.5	7.6 ± 1.4	6.1 ± 2.7	6.7 ± 2.0	7.7 ± 2.5	9.1 ± 3.4	0.1129	**0.0241**	**0.0131**	0.5530	0.9781	0.4868	0.4168
Total Work (mJ)	7.6 ± 2.2	8.6 ± 2.8	9.9 ± 4.1	9.7 ± 1.3	8.0 ± 0	8.7 ± 2.0	9.5 ± 2.3	11.1 ± 3.5	0.1323	**0.0186**	**0.0068**	0.7360	0.8834	0.4816	0.3661

Table 5. Estimated tissue level mechanical properties from 4-point bending of right (non-loaded) and left (loaded) tibiae.

Property	Standard				Thermoneutral				p-value						
	Non-loaded		Loaded		Non-loaded		Loaded		Temp	Load	Treat	Temp x Load	Temp x Treat	Load x Treat	Temp x Load x Treat
	CON	RAL	CON	RAL	CON	RAL	CON	RAL							
Yield Stress (MPa)	182.5 ± 23.9	174.8 ± 13.0	164.2 ± 36.0	167.7 ± 38.3	169.5 ± 18.7	176.9 ± 23.0	159.0 ± 54.8	187.2 ± 48.3	0.8880	0.4435	0.2805	0.8931	0.1219	0.3149	0.2542
Ultimate Stress (MPa)	199.1 ± 19.2	194.3 ± 18.7	206.0 ± 21.1	203.9 ± 17.3	188.6 ± 14.2	202.5 ± 14.9	209.1 ± 33.4	230.1 ± 41.2	0.1577	**0.0040**	**0.0420**	0.1963	**0.0369**	0.1888	0.4190
Failure Stress (MPa)	113.4 ± 48.6	128.2 ± 47.1	153.6 ± 36.7	131.5 ± 35.8	104.9 ± 36.6	118.4 ± 33.6	149.0 ± 53.3	179.8 ± 66.3	0.6870	**0.0016**	0.2987	0.1727	0.1084	0.9337	0.1240
Ultimate Strain (mε)	25.0 ± 4.2	25.0 ± 1.7	33.0 ± 5.5	29.7 ± 4.8	25.2 ± 2.5	26.4 ± 2.4	33.0 ± 6.0	32.3 ± 10.7	0.1782	**<0.0001**	0.6817	0.9632	0.7153	0.2115	0.6372
Strain to Yield (mε)	21.0 ± 5.6	19.5 ± 1.9	20.7 ± 4.0	20.2 ± 4.6	19.6 ± 0	19.3 ± 1.7	19.3 ± 6.0	18.8 ± 2.5	0.2632	0.3884	0.3821	0.2338	0.9885	0.4926	0.6921
Total Strain (mε)	60.5 ± 19.5	61.1 ± 17.3	63.8 ± 22.4	63.4 ± 8.4	65.6 ± 25.2	59.3 ± 12.7	63.4 ± 9.6	61.9 ± 9.5	0.4144	0.9729	0.8663	0.9224	0.1830	0.5205	0.9031
Modulus (GPa)	9.9 ± 1.3	10.2 ± 1.4	8.8 ± 1.2	9.3 ± 1.2	9.7 ± 0.8	10.3 ± 0.9	9.4 ± 2.6	11.3 ± 3.3	0.2525	0.0894	**0.0059**	0.0961	**0.0234**	**0.0412**	0.3124
Resilience (MPa)	2.1 ± 0.9	1.8 ± 0.2	1.9 ± 0.7	1.9 ± 0.8	1.8 ± 0.4	1.8 ± 0.4	1.7 ± 0.9	1.9 ± 0.5	0.6434	0.6345	0.9011	0.5419	0.5535	0.9409	0.6230

Significant Post-hoc Tukey Comparisons

Ultimate Stress	**p-value**
Standard: Non-loaded, CON vs Thermoneutral: Loaded, RAL	0.0107
Standard: Non-loaded, RAL vs Thermoneutral: Loaded, RAL	0.0023
Thermoneutral: Non-loaded, CON vs Thermoneutral: Loaded, RAL	<0.0001
Thermoneutral: Non-loaded, RAL vs Thermoneutral: Loaded, RAL	0.0315
Thermoneutral: Loaded, CON vs Thermoneutral: Loaded, RAL	0.0293
Modulus	**p-value**
Standard: Loaded, CON vs Thermoneutral: Loaded, RAL	0.0052
Standard: Loaded, RAL vs Thermoneutral: Loaded, RAL	0.0402
Thermoneutral: Loaded, CON vs Thermoneutral: Loaded, RAL	0.0020

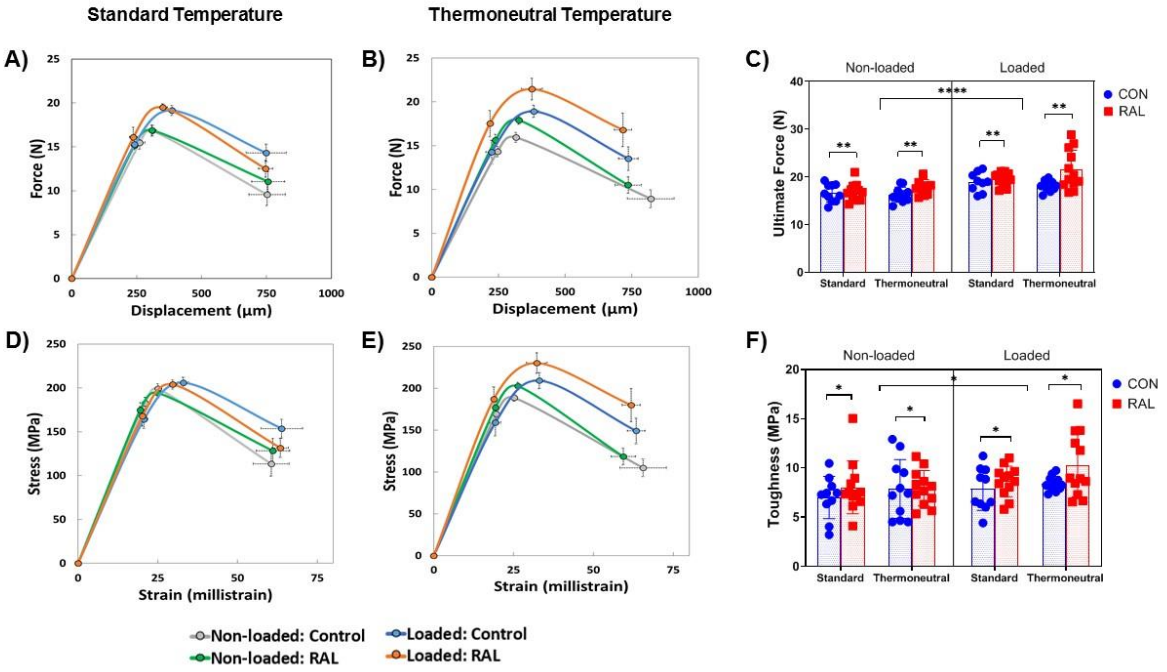

Figure 4. Mechanical properties of the right and left tibiae; standard-CON (n=10), standard-RAL (n=12), thermoneutral-CON (n=11), thermoneutral-RAL (n=12). **A)** Average force-displacement plot for standard temperature, showing stronger loaded bones. **B)** The strength disparity continued at the thermoneutral temperature as quantified by **C)** the ultimate force. **D)** Average stress-strain plots for mice housed at standard temperature show how tissue-level properties increase with loading and RAL, **E)** with similar results at thermoneutral temperature. **F)** Bone toughness increases with loading and RAL treatment. **** $p<0.0001$, ** $p=0.0092$, * $p\leq0.05$.

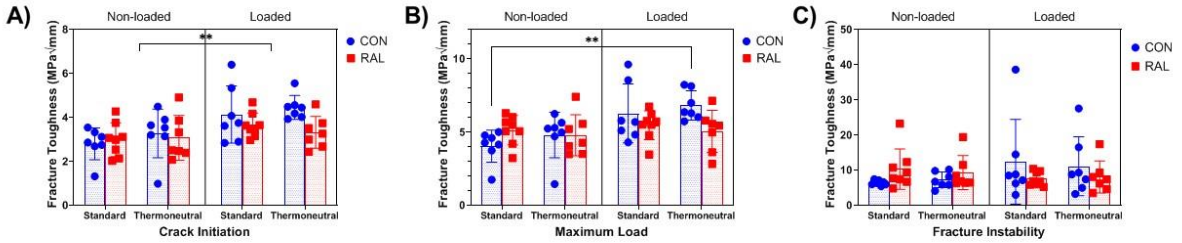

Figure 5. Fracture toughness stress intensity factors for **A)** crack initiation, **B)** maximum load, and **C)** fracture instability. Loading increased crack initiation (** $p=0.0012$) and thermoneutral: loaded, CON increased from standard: non-loaded, CON (** $p=0.0069$). Standard-CON (n=7), standard-RAL (n=8), thermoneutral-CON (n=7), thermoneutral-RAL (n=8).

4. CONCLUSION

4.1 Discussion

Targeted tibial loading is a common non-invasive external loading method that has been shown to induce a robust bone formation response. Previous work from our group has shown that a significant 15% increase in cortical thickness is possible after only two weeks of loading female C57BL/6J mice to 2050με. [30] By extending the loading duration to 6 weeks, an average cortical thickness increase of 26% was observed at the tibial mid-shaft. [23] The extended 6 week timeframe was chosen for this study to allow time to observe a potential additive effect of loading and RAL. As a result, we observed a strong effect on both geometric architecture and cortical properties due to loading in the current study. There were clear and robust mass-based improvements in each architectural property investigated in both cancellous and cortical regions. The only exception was that cortical tissue mineral density was decreased by loading, while trabecular tissue mineral density was increased. This can likely be explained by the difference in the rate at which trabecular and cortical bone respond to loading. The trabecular formation response is faster, so the new bone would have had extra time to mineralize after forming. The cortical response is more robust and, therefore, may be drawn out over a longer time period. The new cortical bone that was formed due to loading had less time to mineralize resulting in a lower overall tissue mineral density. Loading clearly increased bone formation because the proximal-mid bone area and cortical thickness increased by 15% and 10% at standard temperatures and 16% and 11% at thermoneutral temperatures, respectively. The increase in thickness was smaller than shown in previous studies, but this could be attributed to the different anatomical location where the properties were determined. The bone volume fraction in cancellous bone was increased by 26% and 31% in standard and thermoneutral temperatures, respectively. This increase was driven by an increase in trabecular thickness and number and accompanied by a decrease in trabecular spacing.

The mass-based improvements due to loading translated to increased whole bone mechanical properties. Loading shifted the force-displacement curve up which increased the maximum and failure forces and also increased the postyield work and total work. The improvements to postyield work and total work were more modest compared to the other loading

effects, but this could be attributed to the higher variability in post-yield properties. [34] Not only were ultimate and failure forces increased, but so were the stresses which indicates that improvements were not solely mass-based and perhaps tissue quality was also improved. Similarly to total work, toughness was improved but was a more modest change. Fracture toughness is a more direct measure of the tissue behavior and fracture resistance since it tests the ability of the tissue to resist the initiation and propagation of cracks. The increase in crack initiation and maximum load stress intensity factors are further indicators of the improved bone tissue quality.

Raloxifene is known to control bone resorption by binding to osteoblasts and activating the estrogen receptor. Another non-cellular mechanism of action is raloxifene's ability to bind to collagen in the bone matrix and enhance tissue hydration which could explain how the drug is capable of reducing fracture risk in osteoporosis patients. Raloxifene's ability to improve tissue quality could be reflected in architectural and mechanical improvements if administered during an active bone formation response. Previous work from our group demonstrated combination effects of loading and raloxifene in female mice, but the effects were less pronounced than predicted. [23] The current study displayed similar effects, providing further support for the potential of combination treatments for advanced improvements. In this case, loading drove the improvements, yet raloxifene still improved both the cancellous and cortical architecture. Raloxifene improved every property investigated in cancellous bone, but the effects in cortical bone were more modest. Large sample sizes and the power that comes with the 3-way ANOVA analysis may also have boosted the raloxifene effects that were seen compared to previous work. Treatment had a milder impact on bone mechanics. Elastic modulus was increased only by raloxifene treatment. This is in contrast to the tissue hydration mechanism of the drug. The increased bound water content within the bone matrix should make the tissue less stiff as it allows for more efficient load transfer from the mineral to the collagen. The increased modulus, along with other mechanical properties, was a modest change that may be attributed to the large sample sizes and requires further investigation.

The novelty of this study was the addition of altered housing temperature. Thermoneutral housing was investigated with the expectation that the removal of cold stress that is imposed upon animals housed at standard temperatures would allow for extra energy that could be utilized towards a response that would accentuate the impacts of loading and raloxifene. Surprisingly, thermoneutral housing failed to have any major effects in either trabecular or cortical architecture and had no impact on mechanical properties or fracture resistance. The few effects of temperature

which were detected were actually detrimental to cortical geometry. Temperature impacted the overall size of the bone (bone area, cortical thickness, and I_{max}) which suggests a delay in growth based expansion. It is interesting to note that aside from these few cortical effects, temperature's only other effect was to decrease trabecular thickness. It should also be noted that this was a large study with 80 animals, so the modest changes that were observed due to temperature could have been driven by the high number of samples that were being analyzed. Large sample sizes and the 3-way ANOVA analysis, which pools samples across groups for main effect analyses, may also have boosted the effects of raloxifene as noted above. Mice housed at thermoneutral conditions responded to mechanical loading in almost the same manner as those housed under standard room temperature conditions, indicating that further mechanical loading research in bone can take place at standard temperatures (22°C) without fear of mechanical or morphological end points being affected.

4.2 Limitations and Future Work

Our study showed that housing temperature did not have an effect on bone morphology or mechanical properties when mice were subjected to either mechanical loading or pharmaceutical treatment, yet other studies with thermoneutral housing in mice have shown greater effects. One study demonstrated that thermoneutral housing (32°C) prevented premature cancellous bone loss in female C57BL/6J mice. [23] This study was investigating bone loss and was, therefore, much longer than ours (14 weeks for the C57Bl/6 mouse model and 18 weeks for the C3H mouse model vs our 6 week study). The bone loss that occurs from 8 weeks of age (peak cancellous bone mass) until the age of 18-22 weeks (peak bone mass) is significant and could offer a greater opportunity for the metabolic boost that we were expecting to see in our study to actually have an effect and improve architecture. Interestingly, this group did not observe any robust differences in bone length or cortical architecture, similar to our study. Other work in osteoporotic mice also showed improved trabecular bone without improvements in cortical bone in mice exposed to higher housing temperatures. [35] The mass-based trabecular improvements translated to mechanical improvements in the yield point and ultimate force in the femur as tested in three-point bending. Main differences between this study and the current study are the disease state model, higher temperature housing (34°C), and older mice (16 weeks to 24 weeks). It seems that the osteoporotic model provides another opportunity for the extra energy that is being conserved in thermoneutral

conditions to be utilized towards an improved response. Future work in different ages, disease models, and organ systems may be necessary to extend the findings of this study.

There were other limitations to the current study. Female mice were chosen intentionally due to the clinical relevance of raloxifene treatment, however, in future studies it may be important to assess the impact of housing temperature on both sexes. A strain calibration was run prior to the study to determine the maximum load necessary to induce a tensile strain of 2050 με. Loading to the same maximum load throughout the 6 week study assumes that the strain stays constant, but strain would change as the bone changes with loading, treatment, and age so that the different groups would eventually see different strains when loading to the same force. Future studies may need to include a second strain calibration on a subset of mice from each group during the study to adjust load levels. There are also limitations with raloxifene as a clinical treatment. While raloxifene has proven efficacious in improving bone quality, the estrogenic therapy can produce adverse effects such as hot flashes or increased thrombosis risk. The estrogen receptor binding also prevents raloxifene from being used in at-risk patients, including children. [36,37]

In summary, combined effects of external loading and raloxifene on bone morphology and mechanical properties were demonstrated. Thermoneutral housing failed to influence these findings. Future work will aim to consider the effect of thermoneutral housing in disease states so that the temperature may provide that metabolic boost that was expected to further enhance the combined effect of loading and raloxifene.

LIST OF REFERENCES

1. D. B. Burr and O. Akkus, *Chapter 1 – Bone Morphology and Organization*. San Diego: Academic Press, 2014, pp. 3-25.

2. M. C. van der Meulen, K. J. Jepsen, and B. Mikic, "Understanding bone strength: size isn't everything," *Bone*, vol. 29, no. 2, pp. 101-4, 2001.

3. A. Taranta, M. Brama, A. Teti, R. Scandurra, G. Spera, D. Agnusdei, et al., "The selective estrogen receptor modulator raloxifene regulates osteoclast and osteoblast activity in vitro," *Bone*, vol. 30, pp. 368-76, 2002.

4. H. U. Bryant, Mechanism of action and preclinical profile of raloxifene, a selective estrogen receptor modulation," *Rev Endocr Metab Disord*, vol. 2, no. 1, pp. 129-38, Jan 2001.

5. B. Ettinger, D. M. Black, B. H. Mitlak, R. K. Knickerbocker, T. Nickelsen, H. K. Genant, C. Christiansen, P. D. Delmas, J. R. Zanchetta, J. Stakkestad, C. C. Gluer, K. Krueger, F. J. Cohen, S. Eckert, K. E. Ensrud, L. V. Avioli, P. Lips, and S. R. Cummings, "Reduction of vertebral fracture risk in postmenopausal women with osteoporosis treated with raloxifene: results from a 3-year randomized clinical trial," *JAMA*, vol. 282, no. 7, pp. 637-45, 1999.

6. E. Seeman, G. G. Crans, A. Diez-Perez, K. V. Pinette, and P.D. Delmas, "Anti-vertebral fracture efficacy of raloxifene: a meta-analysis," *Osteoporosis international*, vol 17, pp. 313-16, 2006.

7. M. R. Allen, K. Iwata, M. Sato, and D. B. Burr, "Raloxifene enhances vertebral mechanical properties independent of bone density," *Bone*, vol 39, pp. 1130-5, 2006.

8. M. R. Allen, H. A. Hogan, W. A. Hobbs, A. S. Koivuniemi, M. C. Koivuniemi, and D. B. Burr, "Raloxifene Enhances Material-Level Mechanical Properties of Femoral Cortical and Trabecular Bone," *Endocrinology*, vol. 148, pp. 3908-13, 2007.

9. M. Aref, M. A. Gallant, J. M. Organ, J. M. Wallace, C. L. Newman, D. B. Burr, et al., "In vivo reference point indentation reveals positive effects of raloxifene on mechanical properties following 6 months of treatment in skeletally mature beagle dogs," *Bone*, vol. 56, p. 10.1016/j.bone.2013.07.009, 07/17 2013.

10. N. Bivi, H. Hu, B. Chavali, M. J. Chalmers, C. T. Reutter, G. L. Durst, et al., "Structural features underlying raloxifene's biophysical interaction with bone matrix," *Bioorganic & medicinal chemistry*, vol. 24, pp. 759-67, 2016.

11. M. A. Gallant, D. M Brown, M. Hammond, J. M. Wallace, J. Du, A. C. Deymier-Black, et al., "Bone cell-independent benefits of raloxifene on the skeleton: a novel mechanism for improving bone material properties," *Bone,* vol. 61, pp. 191-200, 2014.

12. M. R. Allen, M. W. Aref, C. L. Newman, J. R. Kadakia, and J. M. Wallace, "El Raloxifeno invierte fragilidad Ósea inducida por el tratamiento anti-remodelación y aumenta la resistencia a la fatiga a través de mecanismos mediados no celulares," Actualizaciones en Osteologia, vol. 12, pp. 169-179, 2016.

13. N. Dalen, and K. E. Olsson, "Bone mineral content and physical activity," *Acta Orthop Scand,* vol. 45, pp. 170-4, 1974.

14. R. L. Wolman, L. Faulmann, P. Clark, R. Hesp, and M. G. Harries, "Different training patterns and bone mineral density of the femoral shaft in elite, female athletes," *Ann Rheum Dis,* vol. 50, pp. 487-9, Jul 1991.

15. V. Brewer, B. M. Meyer, M. S. Keele, S. J. Upton, and R. D. Hagan, "Role of exercise in prevention of involutional bone loss," *Med Sci Sports Exerc,* vol. 15, pp. 445-9, 1983.

16. R.K. Fuchs, J. J. Bauer, and C. M. Snow, "Jumping improves hip and lumbar spine bone mass in prepubescent children: a randomized controlled trial," *J Bone Miner Res,* vol. 16, pp. 148-56, Jan 2001.

17. D. B. Burr and O. Akkus, *Chapter 11 – Mechanical Adaptation*. San Diego: Academic Press, 2014, pp. 206-9.

18. C. J. Gordon, "Thermal physiology of laboratory mice: Defining thermoneutrality," *Journal of Thermal Biology*, vol. 37, pp. 654-85, 2012.

19. F. Claire Hankenson, J. O. Marx, C. J. Gordon, and J. M. David, "Effects of Rodent Thermoregulation on Animal Models in the Research Environment," *Comparative Medicine*, vol. 68 (6), pp. 425-38, 2018.

20. V. Glatt, E. Canalis, L. Stadmeyer, M. L. Bouxsein, "Age-related changes in trabecular architecture differ in female and male C57BL/6J mice," *J Bone Mineral Res: Off J Am Soc Bon Mineral Res*, vol 22. Pp. 1197-1207, 2007.

21. U. T. Iwaniec, K. A. Philbrick, C. P. Wong, J. L. Gordon, A. M. Kahler-Quesada, D. A. Olson, A. J. Branscum, J. L. Sargent, V. E. DeMambro, C. J. Rosen, and R. T. Turner, "Room temperature housing results in premature cancellous bone loss in growing female mice: implications for the mouse as a preclinical model for age-related bone loss," *Osteoporosis Int*, vol. 27, pp. 3091-3101, 2016.

22. S. A. Martin, K. A. Philbrick, C. P. Wong, D. A. Olsen, A. J. Branscum, D. B. Jump, C. K. Marik, J. M. DenHerder, J. L. Sargent, R. T. Turner, and U. T. Iwaniec, "Thermoneutral housing attenuates premature cancellous bone loss in male C57BL/6J mice," *Endocrine Connections*, vol. 8, no. 11, pp. 1455-67, 2019.

23. A. G. Berman, J. D. Damrath, J. Hatch, A. N. Pulliam, K. M. Powell, M. Hinton, J. M. Wallace, "Effects of Raloxifene and Targeted Tibial Loading on Bone Mass and Mechanics in Male and Female Mice," Submitted, *Bone,* 2020.

24. R. L. De Souza, M. Matsuura, F. Eckstein, S. C. Rawlinson, L. E. Lanyon, and A. A. Pitsillides, "Noninvasive axial loading of mouse tibiae increases cortical bone formation and modifies trabecular organization: a new model to study cortical and cancellous compartments in a single loaded element," *Bone*, vol. 37, pp. 810-8, 2005.

25. J. C. Fritton, E. R. Myers, T. M. Wright, and M. C. H. van der Meulen, "Loading induces site specific increases in mineral content assessed by microcomputed tomography of the mouse tibia," *Bone* vol. 36, pp. 1030-8, 2005.

26. A. M. Weatherholt, R. K. Fuchs, and S. J. Warden, "Cortical and trabecular bone adaptation to incremental load magnitudes using the mouse tibial axial compression loading model," *Bone*, vol. 52, pp. 372-9, 2013.

27. M. R. Allen, H. A. Hogan, W. A. Hobbs, A. S. Koivuniemi, M. C. Koivuniemi, and D. B. Burr, "Raloxifene enhances material-level mechanical properties of femoral cortical and trabecular bone," *Endocrinology*, vol. 148, no. 8, pp. 3908-13, 2007.

28. M. R. Allen, P. R. Territo, C. Lin, S. Persohn, L. Jiang, A. A. Riley, B.P. McCarthy, C. L. Newman, D. B. Burr, and G. D. Hutchins, "In vivo ute-mri reveals positive effects of raloxifene on skeletal-bound water in skeletally mature beagle dogs," *J Bone Miner Res*, vol. 30, no. 8, pp. 1441-4, 2015.

29. A. G. Berman, J. M. Wallace, Z. R. Bart, and M. R. Allen, "Raloxifene reduces skeletal fractures in an animal model of osteogenesis imperfecta," *Matrix Biol*, vol. 52-54, pp. 19-28, 2016.

30. A. Berman, C. Clauser, C. Wunderlin, M. A. Hammond, J. M. Wallace, "Structural and Mechanical Improvements to Bone are Strain Dependent with Axial Compression of the Tibia in Female C57BL/6 Mice," *PloS One*, vol. 10, no. 6, p. e0130504, 2015.

31. J. M. Wallace, K. Golcuk, M. D. Morris, and D. H. Kohn, "Inbred strain-specific response to biglycan deficiency in the cortical bone of C57BL6/129 and C3H/He mice," *J Bone Miner Res*, vol. 24, no. 6, pp. 1002-12, 2009.

32. R. O. Ritchie, K. J. Koester, S. Ionova, W. Yao, N. E. Lane, and r. Ager, J. W., "Measurement of the toughness of bone: a tutorial with special reference to small animal studies," Bone, vol. 43, no. 5, pp. 798-812, 2008.

33. M. A. Hammond, A. G. Berman, R. Pacheco-Costa, H. M. Davis, L. I. Plotkin, and J. M. Wallace, "Removing or truncating connexin 43 in murine osteocytes alters cortical geometry, nanoscale morphology, and tissue mechanics in the tibia," *Bone*, vol. 88, pp. 85-91, 2016.

34. J. D. Currey, J. W. Pitchford, and P. D. Baxter, "Variability of the mechanical properties of bone, and its evolutionary consequences," *J R Society*, vol. 4, no. 12, pp. 127-135, 2007.

35. C. Chevalier et al., "Warmth Prevents Bone Loss Through the Gut Microbiota," *Cell Metabolism*, vol. 32, pp. 1-16, 2020.

36. A. Qaseem, M. A. Forciea, R. M. McLean, and T. D. Denberg, "Treatment of low bone density or osteoporosis to prevent fractures in men and women: A clinical practice guideline updated from the American college of physicians," *Ann Intern Med*, vol. 166, no. 11, pp. 818-39, 2017.

37. I. R. Reid, "Efficacy and effectiveness and side effects of medications used to prevent fractures," *J Intern Med*, vol. 277, no. 6, pp. 690-706, 2015.